

A revised manuscript submitted for consideration to publish in
International Journal of Heat and Mass Transfer

HYDRODYNAMICS AND HEAT TRANSFER IN BUBBLY FLOW IN THE TURBULENT BOUNDARY LAYER

Dariusz Mikielewicz

Technical University of Gdańsk, Faculty of Mechanical Engineering
ul. Narutowicza 11/12, 80-952 Gdańsk

Summary

In the work presented is a new approach to modelling the bubbly flow in the boundary layer. The approach is based on summation of dissipation energy coming from the shearing turbulent flow in the absence of bubbles and the dissipation contribution from the presence of bubbles. As a result we obtain the dissipation of equivalent single phase turbulent flow. The model has been solved using the method of asymptotic correction to provide an explicit differential equation describing the velocity profile. That can be solved with the assumption of constant void fraction distribution to yield the analytical velocity profile. Alternatively, author has developed his own model of lateral void migration, which is distinct from other models by virtue of presence of another rotational velocity. Velocity distributions calculated using the new model have been compared against the experimental data of turbulent bubble flows with small void fraction. A good consistency between calculations performed using a new model and available experimental data has been obtained. Additionally, a solution of the temperature field is also given. In the case of a constant void fraction distribution analytical distribution of the Nusselt number is given or the set of differential equations needs to be solved.

NOMENCLATURE

- α - void fraction
- d_b - bubble diameter
- D - bubble diffusivity

δ - layer thickness
e - dissipation energy
F - force acting on a bubble
g - gravity
 κ - von Karman constant
n - number of bubbles
N - dissipation power
 ρ - density
 μ - turbulent viscosity
 τ - shear stress
T - temperature
u, θ - longitudinal and transverse velocity
V - volume
y - transverse co-ordinate

Subscripts

b - bubble
D - drag
e - equivalent
l - liquid, linear
n - non-linear
R - relative bubble to liquid
t - turbulent
TP - two-phase
w - wall

1. INTRODUCTION

Correct modelling of the gas phase distribution is of primary importance for pressure drop predictions as well as heat and mass transfer calculations. Bearing in mind, that two-phase flow mechanisms are governed by multidimensional effects, which occur at specific flow regimes of bubbly flow it is so difficult to capture the physics of such behaviour. In the case of upward bubbly flow there can be found two distinct distributions of void fraction, one form which peaks in the core of the flow, i.e. the so called phenomenon of “core peaking”, and a case with a peak close to the wall, named the “wall peaking”. Influences of void fraction peaking on heat transfer cause significant modelling problems. Several multidimensional mechanisms have been proposed to explain such behaviour, however so far none of them has proved to be successful.

A great deal of effort has been devoted to the development of models capable of describing two-phase flows, Drew and Wallis [1]. Calculations of velocity distributions and modelling of interfacial phenomena in the flows with dispersed phase show numerous constraints of such models, Lance and Lopez de Bertodano [2]. These constraints stem primarily from the fact that inappropriate closure equations have been assumed, which describe the momentum exchange at the interface and turbulence of each phase. The closure equations have either no correct physical meaning or the mechanisms describing the phenomena are not accurately captured. Complexity of problems concerned with two-phase flows renders that the solutions are sought by all possible means, such as generalisation of the results of experimental investigations, theory of similarity and theoretical investigations. The most appropriate at the moment model is the four field two fluid model, Lahey and Drew [3], but even that model, despite its undisputed successes in simulations of vertical flows in ducts, free external flows or subcooled boiling, the four field two fluid model still requires research into the fundamental issues of physical phenomena governing the flow. Analysis of the phenomena occurring in the two-phase flow is a very difficult task due to the complexity of the phenomena under consideration. On the other hand, usage of the four field two fluid model requires calculations using modern CFD solvers such as for example PHOENICS, CFX or purpose written software.

In the literature on two-phase flows there can be found a number of experimental data, which have been conducted in order to understand better the structure of a turbulent bubble flow. Serizawa et al. [4], Wang et al. [5], Nakoryakov et al. [6], Liu [7] analysed the bubbly

flow, where the main turbulence changes and void fraction distributions took place in the vicinity of the wall. These research has, however, been done for the case of flows in pipes, where due to rather small pipe diameters the measurements and their interpretation was quite difficult. Recently, there appeared a new study of the bubble flow in the boundary layer on a flat plate due to Moursali et al. [8], Marie et al. [9]. This detailed data is concerned with a much simpler configuration, namely that of a turbulent boundary layer developing on a vertical flat plate immersed in a uniform upward bubbly flow and this data has been chosen for validation of the presented model.

As known, the solution to heat transfer in the fully developed single phase boundary layer flow is a universal velocity and temperature field. The aim of the present work is to present a similar solution for the case of fully developed bubbly flow in the boundary layer. This is by no means simple problem which requires prior knowledge of the velocity field, i.e. velocity profile and void fraction distribution in the boundary layer. The author has developed his own concept of modelling of two-phase flow in the boundary layer, Mikielwicz [10, 11], which in the case of a constant void fraction gives an analytical form of velocity distribution. Such model of the hydrodynamics of bubble flow can be subsequently used to obtain the temperature field. The temperature field can be obtained in a twofold manner. Firstly, it will be derived for the case of a constant void fraction in the boundary layer. Secondly, own model for a variable void fraction across the boundary layer, Mikielwicz [12], will be used in resolution of the temperature field. In this case it is necessary to solve three ordinary differential equations of the first order. Results of calculations have been compared against the limiting case of theoretical correlations describing the flow over the plate by the viscous single phase fluid. Obtained have been satisfactory results.

2. MODEL OF A TURBULENT TWO PHASE FLOW

Firstly presented will be the model of the bubbly flow. It is derived based on energetical considerations of the dissipation process in the two-phase bubbly flow. The following assumptions have been made:

1. Turbulence exists only in the liquid phase.
2. Dispersed phase (spherical bubbles) occupy some volume of the flow and influence the momentum and turbulence of liquid phase.

3. There is no motion of the gaseous phase inside the bubbles.
4. Fluid motion is fully developed.
5. Surface void fraction is equal to volumetric void fraction.

A general flow schematic is presented in Fig. 1. The problem is considered as one-dimensional. We consider a control volume V containing a number of vapour bubbles n . The underlying hypothesis for derivation of the new model of bubbly flow is a postulate that the total dissipation energy in the flow is a sum of dissipation coming from the shearing liquid flow and dissipation from the bubbles generating the dissipation, which in the specific form yields:

$$e_e = e_{TP} + e_b \quad (1)$$

Dissipation energy of the two-phase flow can be defined as a power lost due to friction by an arbitrary layer isolated from the velocity profile, of the thickness δ and area S , with respect to the control volume (see Fig. 2).

After some re-arrangements, the dissipation of the flow in the control volume is expressed as a ratio of the square of the shear stress in the continuous liquid phase to the turbulent viscosity:

$$e_{TP} = \frac{N_{TP}}{V} = \frac{\tau_{TP} S u_{TP}}{S \delta} = \frac{\tau_{TP} u_{TP}}{\delta} = \frac{\tau_{TP}^2}{\mu_t} = \frac{(1-\alpha)^2 \tau_l^2}{\mu_t} \quad (2)$$

where τ_{TP} describes the shear stress in two-phase flow and $\tau_l = \mu_l \partial u_l / \partial y$ is the shear stress in liquid. As can be seen, the shearing flow influence is modelled by the quantities related to the liquid flow.

The specific energy dissipation from the bubbles is defined as a ratio of power dissipated by the bubbles in the control volume. The dissipation power can be expressed as a product of the total force acting on the bubbles and the relative bubble velocity. The total force acting on the bubble in the present state of work will be expressed as an aerodynamic force. Using the above assumptions, the equation expressing the energy dissipation due to the presence of bubbles takes a form:

$$e_b = \frac{N}{V} = \frac{n F_b u_R}{V} = \frac{3 \alpha \rho_l C_D u_R^3}{4 d_b} = \frac{\tau_b^2}{\mu_t} \quad (3)$$

where $F_b = C_D \frac{\rho_l u_R^2}{2} \frac{\pi d_b^2}{4}$; $V = \frac{\pi d_b^3}{6}$ and τ_b is the stress resulting from the presence of bubbles.

Finally, we assume the idea of the equivalent two-phase flow, which is regarded as a flow with single phase properties corresponding to the properties of two-phase flow. Dissipation of the equivalent flow in the control volume of arbitrary layer isolated from the flow can be written analogically to (3) as:

$$e_e = \frac{\tau_e^2}{\mu_t} \quad (4)$$

The turbulent viscosity appearing in the model is modelled using the Prandtl mixing length model. In our analysis we will also use the following quantities required in reduction of equations to the non-dimensional form:

$$u_\tau = \sqrt{\frac{\tau_w}{\rho}} \quad u^+ = \frac{u_t}{u_\tau} \quad y^+ = \frac{y u_\tau}{\nu} \quad \tau_e^+ = \frac{\tau_e}{\tau_w} \quad T^+ = \frac{T}{T_\infty} \quad (5)$$

Substituting (2), (3) and (4) into (1) we obtain a relation linking the shear stress in the two-phase flow with turbulent stresses of continuous phase and energy of dissipation from the presence of bubbles, i.e. the model of two-phase flow. Substituting the Prandtl mixing length model for the turbulent viscosity and casting the whole expression into a non-dimensional form we get:

$$\frac{\tau_e^{+2}}{\kappa^4} = (1-\alpha)^2 y^{+4} \left(\frac{du^+}{dy^+} \right)^4 + M \alpha y^{+2} \left(\frac{du^+}{dy^+} \right) \quad (6a)$$

where M is defined as:

$$M = \frac{3}{4} \frac{C_D u_R^3}{d_b \kappa^2} \frac{\nu}{u_\tau^4} \quad (6b)$$

Equation (6a) is a highly non-linear equation of the first order, which can only be solved numerically. However, it obeys the asymptotic condition, i.e. when the void fraction, $\alpha=0$, we have a single phase flow of liquid alone. The above result can be cast into a more general form which describes another very important issue, i.e. that the stress in the two-phase flow is

a sum of the squares of stresses coming from the shear stress in liquid without the presence of bubbles and interaction of bubbles on the liquid. This is a geometrical summation rather than the algebraic one, often quoted in the literature:

$$\tau_e^2 = \tau_{TP}^2 + \tau_b^2 \quad (7)$$

Relation (7) stems directly from (1) if substituted are expressions (2), (3) and (4). It forms therefore the extension of acknowledged so far assumptions made by other authors, who regarded that stresses are linearly dependent, Lance et al. [13]. The assumption of a linear relation between the shear stress coming from the shearing liquid flow and the bubbles is the simplest of all assumptions and in reality is always valid for infinitely small change of parameters. In a wider range of variation of parameters a non-linear behaviour appears. Postulated hypothesis (1) results with a geometric summation of stresses (7), hence shows the theoretical foundations of the model, which are quite different from the ones hitherto assumed. Asymptotic analysis of (7) gives the following: if the term $\tau_e/\tau_b \rightarrow \infty$ then $\tau_e \rightarrow \tau_b$, whereas in the case when $\tau_e/\tau_b \rightarrow 0$ then $\tau_e \rightarrow \tau_{TP}$. Such relation exhibiting the non-linear behaviour of equivalent stress cannot be obtained with linear assumption of stress variation.

3. UNIVERSAL VELOCITY PROFILE FOR BUBBLE FLOW

It is generally acknowledged that the numerical methods cannot provide an analytical form of the solution, which is much more useful for discussion than tabulated data or graphs; same pertains to the generality of the solution obtained in this way. In this light an attempt has been made to provide an approximate solution of equation (6a) valid in the entire range of considered void fraction. The method of solution is based on the method of asymptotic correction, Polyanin and Dilman [14]. Asymptotic correction allows us to effectively improve various approximate formulas obtained earlier from both theoretical considerations and experimental data using the exact asymptotes of the original boundary problem. Applying this method to (6a) the following formulae describing the velocity gradient in a two-phase boundary layer can be obtained [11]:

$$\frac{du^+}{dy^+} = \frac{1}{\kappa y^+ (1-\alpha)^{1/2} + M \kappa^4 \alpha y^{+2}} \quad (8)$$

Equation (8) is an ordinary differential equation. When we could assume a constant void fraction distribution then (8) has a following analytical solution:

$$u^+ = -\frac{1}{\kappa(1-\alpha)^{1/2}} \ln \frac{\kappa(1-\alpha)^{1/2} + M\alpha\kappa^4 y^+}{y^+} + C \quad (9)$$

Equation (9) can be regarded as the law of the wall for two-phase bubble flows. In order to determine the integration constant C we need to assume some division of the two-phase flow into regimes. Due to the fact that the structure of the two-phase flow is yet to be satisfactorily understood, it has been assumed in the present work that the division of the flow similar to the single phase flow holds. In some literature there is assumed that the non-dimensional thickness of the laminar sublayer extends to $y^+=11.6$, Troshko and Hassan [15]. In the present case, it has been assumed that in the laminar sublayer, of the assumed thickness $y^+=8$, there are no bubbles and then the constant C is determined to be $C=7.7$ for $\kappa=0.4$.

4. MECHANISM OF LATERAL MOTION OF BUBBLES

The correct solution to equation (8) should contain the relation describing the void fraction distribution across the boundary layer. This task is by no means simple. So far several researchers have dealt with this problem, however without much success. It has been acknowledged that the mechanism of lateral migration of bubbles in the vicinity of the wall stems from the balance of lateral and drag forces, Moraga et al. [16].

Horizontal forces acting on the bubble have schematically been presented in Fig. 1. It must be noted that the bubble is considered here as a gas bubble surrounded by a thin layer of liquid. Such approach requires consideration of contribution of the added mass effect. The added mass effect is considered here both in the translative lateral motion of the bubble as well as the bubble's rotating motion [17].

In order to consider the bubble lateral motion in the work considered is a fully developed bubbly flow under steady-state conditions. In this case vertical forces are neglected in derivation of the lateral motion. It is assumed that the lift force F_L is balanced by the lateral drag force F_D and the inertia force. The bubble inertia force in the lateral translative motion has been included here and the force balance on the bubble therefore takes the form:

$$m_b \frac{d \mathcal{G}_b}{d t} = F_L - F_D \quad (10)$$

where m_b is a bubble virtual mass, which is modelled as a half of the mass of displaced liquid, see Fig. 1. Mass of displaced liquid has been calculated [11] as a thin layer of liquid surrounding the bubble of thickness δ . Sought added mass is then equal to $\rho_l \pi d_b^3 / 12$. Additionally, in (10) \mathcal{G}_b is a lateral bubble velocity. In the one-dimensional steady state flow the lift force can be expressed in the form:

$$F_L = C_L \frac{\pi}{6} \rho_l d_b^3 u_R \omega \quad (11)$$

The relative bubble velocity, u_R , is approximated by the bubble terminal rise velocity in the quiescent container, $u_R = u_b - u_l \approx u_\infty$. Such relation is applicable in the case of small void fractions. The angular velocity of considered bubble resulting from the velocity field is

$$\omega = \frac{2 \Delta u_l}{d_b} \cong 2 \frac{\partial u_l}{\partial y}. \text{ The lift coefficient was assumed a constant value of } C_L = 0.1.$$

There is however another influence on the bubble rotation, which has yet to be considered in the literature. It is caused by the fact that the bubble in vertical upward motion releases some space behind it, which is subsequently filled by the liquid pushed away by the bubble from its front [12], Fig. 3. If we consider n bubbles in a given control volume travelling upwards, then we can assume that each bubble occupies an imaginary channel of the area of $1/n$, Madejski [18]. These channels have different cross-sectional areas due to the fact that there is a lateral distribution of dispersed phase in the channel. A continuity equation can be written for a selected plane perpendicular to the flow in the form:

$$u_R dt (1 - \alpha) A_k + \frac{\pi d_b^2}{4} dy = 0 \quad (12)$$

If we define the void fraction in the imagined channel as a ratio of bubble projection area to the area of the subchannel, i.e. in the form $\alpha = \frac{\pi d_b^2}{4 A_k}$ then from equation (12) we can derive the liquid velocity, s , in the direction opposite to the liquid motion $s = dy / dt$

$$s = - \frac{\alpha}{1 - \alpha} u_R \quad (13)$$

On such basis velocity, opposite in direction to the liquid velocity, can be derived, which creates an additional rotation of the bubble defined as [10,11]:

$$\omega_2 = 2 \frac{\partial s}{\partial y} = - \frac{2u_R d_b}{(1-\alpha)^2} \left(\frac{d\alpha}{dy} \right) \quad (14)$$

Additional angular velocity acting on a bubble, which subsequently can be algebraically added to the angular velocity resulting from the velocity profile, depending on the concentration profile, i.e. *wall peaking* or *core peaking*, acts in the same or opposite direction as rotation stemming from the primary velocity profile. In the case of two rotations with opposite signs we can observe the motion in one or another way. Such motion is identified by the bubble diameter contained in u_R , i.e. for a certain range of bubble diameters the motion is towards the wall, whereas in others, towards the core of the flow. This has an experimental confirmation, Žun [19], where it has been concluded that in the range from 0.8 mm to 5 mm there is *wall peaking* in the upward flow, whereas for other diameters the maximum takes place in the location of the core of the flow. The presence of a second rotation should contribute to explanation of such behaviour.

In connection to this fact the resultant circulation in (11) ought to be changed, as now it consists of two components, i.e. $\omega = \omega_1^0 + \omega_2^0$. The total circulation can be cast as follows

$$\omega = \omega_1^0 + \omega_2^0 = \left\{ 2 \frac{du_l}{dy} - \frac{2u_R}{(1-\alpha)^2} \left(\frac{d\alpha}{dy} \right) \right\} \quad (15)$$

5. MODELLING OF ADDED MASS IN ROTATING MOTION

Up to now we have been considering the bubble in inviscid liquid flow. This is not true as in all liquid there are shear stresses acting on the bubble reducing its angular velocity. In this light, the angular velocity needs to be changed. The balance of forces acting on the bubble in its rotating motion can be written as:

$$M_0 + \frac{d}{dt} (J \omega) = 0 \quad (16)$$

where M_0 is a rotation resistance moment, J – moment of gas-liquid system inertia with respect to the centroid, ω - angular velocity of centroid. However, there are other forces acting

on the bubble, but they do not produce a force couple with respect to the centroid. The rotation resistance moment with respect to the centroid has been given by Lamb [20]

$$M_0 = \pi d_b^3 \mu_l \omega \quad (17)$$

where the angular velocity is a resultant velocity acting on the bubble, i.e. in our case it acts on the sum of angular velocities. Referring to Lamb [20] we can conclude that the bubble inertia is increased by the half of the mass of displaced liquid, which subsequently can be expressed as a thin layer of liquid of thickness δ surrounding the bubble, and hence the sought mass is $\rho_l \pi d_b^3 / 12$. If we compare the relations $\pi d_b^2 \delta = \rho_l \pi d_b^3 / 12$ then we obtain the thickness of modelled liquid layer as $\delta = d_b / 12$ [18]. It can be seen that the considered liquid film is very thin. Total moment of inertia of bubble is

$$J = J_b + J_l = \frac{\pi d_b^5 \rho_l}{60} \left(\frac{1}{2} + \frac{\rho_g}{\rho_l} \right) \cong \frac{\pi d_b^5 \rho_l}{120} \quad (18)$$

Lets cast the balance of forces on a bubble in a slightly different form

$$J \frac{d\omega}{dy} \frac{dy}{dt} = -M_0 \quad (19)$$

The derivative dy/dt expresses the bubble lateral velocity, \mathfrak{G}_b . As a result of integration of (19) we can obtain variation of angular velocity with respect to the distance from the wall. This is described by the relation

$$\omega = \omega_0 \exp \left(\frac{\pi d_b^3 \mu_l}{J} \int_0^y \frac{dy}{\mathfrak{G}_b(y)} \right) \quad (20)$$

With the view to see the major trends in the influence of added mass on bubble angular velocity lets assume that the lateral velocity is constant. This assumption is correct for the vast area of the flow. We obtain then the following relation

$$\omega = \omega_0 \exp \left(- \frac{120 \nu_l}{d_b^2 \mathfrak{G}_b} y \right) \quad (21)$$

6. THE MODEL OF VOID FRACTION DISTRIBUTION

Lateral drag force can be written in the form:

$$F_D = C_D A \frac{\rho_l g_b^2}{2} = C_D \frac{\pi d_b^2 \rho_l g_b^2}{8} \quad (22)$$

The drag force will be fully defined when the friction factor will be adequately prescribed in order to determine the lateral force. One needs to remember the fact that the bubble Reynolds number in the lateral motion is based on a lateral velocity rather than the relative velocity (as found in considerations of the axial flow). We will use, however, same empirical formulas to obtain the friction factor C_D . For the bubble Reynolds number from the range $0.5 \div 800$ normally the relation $24 / \text{Re}_b (1 + 0.15 \text{Re}_b^{0.687})$ is used. In the present study we used the above relation for the friction factor with own correction included to account for the change of friction factor in the vicinity of the wall. In some paper such correction is regarded as a wall force. The friction factor takes the form:

$$C_D = \frac{24(1 + 0.15 \text{Re}_b^{0.687})}{\text{Re}_b} \left(1 + \frac{0.02 d_b}{y} \right) \quad (23)$$

In some experimental evidence it has been found that there can be observed the change of sign of the lift force, Moraga et al. [9]. There exist various theories explaining this fact, but in author's opinion, so far none is capable of correctly explaining such behaviour. Bubble deformation is regarded as a most plausible explanation for this fact. Postulated model, which contains two angular velocities is capable of explaining such phenomenon. Change of the sign of lift force is a result of a change of the sign of angular velocity (consisting of two components) which is consistent with the physics of the phenomenon. This can even be done without manual change to the lift coefficient, C_L , which is a very popular explanation to this fact. From (10) we can determine the differential equation describing the distribution of lateral velocity:

$$\frac{d g_b}{d y} = \frac{36 \nu_l (1 + 0.15 \text{Re}_b^{0.687})}{d_b^2} \left(1 + \frac{0.02 d_b}{y} \right) - \frac{4 C_L u_R}{g_b} \left[\frac{d u_l}{d y} - \frac{u_R}{(1-\alpha)^2} \frac{d \alpha}{d y} \right] \quad (24)$$

Expression (24) contains two unknowns, namely g_b and the void fraction α . In order to solve (24) we require additional equation combining these variables, which can be for example the diffusion of bubbles in liquid:

$$\alpha \mathcal{G}_b = -D_b \frac{d\alpha}{dy} \quad (25)$$

where D_b is a local bubble diffusivity. Bankoff [21] extended the Reynolds analogy of turbulent flow onto the case of bubble diffusion stating, that the eddy diffusivity of momentum corresponds to the bubble diffusivity. Subsequently he used the Prandtl mixing length model in order to determine eddy diffusivity

$$\varepsilon = D_b = \kappa^2 y^2 \frac{du_l}{dy} \quad (26)$$

In order to include the effect of added mass in a rotational bubble motion we incorporate a correction for added mass effect derived in [17] to amend the circulation on a bubble :

$$\omega = \omega_1 + \omega_2 = (\omega_1^0 + \omega_2^0) \exp\left(-\frac{120 v_l}{d_b^2 \mathcal{G}_b} y\right) \quad (27)$$

The final differential equation describing the distribution of lateral translational velocity with added mass in translative and rotational motion yields

$$\frac{d\mathcal{G}_b}{dy} = \frac{36 v_l (1 + 0.15 \text{Re}^{0.687})}{d_b^2} \left(1 + \frac{0.02 d_b}{y}\right) - \frac{4 C_L u_R}{\mathcal{G}_b} \left[\frac{du_l}{dy} - \frac{u_R}{(1-\alpha)^2} \frac{d\alpha}{dy}\right] \exp\left(-\frac{120 v_l}{d_b^2 \mathcal{G}_b} y\right) \quad (28)$$

In pure air-water system, the relative velocity of bubbles greater than 1.3 mm can be evaluated, Tomiyama et al. [22]:

$$u_R \cong u_\infty = \sqrt{\frac{2\sigma}{\rho_l d_b} + \frac{(\rho_l - \rho_g)g d_b}{2\rho_l}} \quad (29)$$

In the case of air bubbles migrating in water this relation gives a velocity equal to 0.23 m/s.

7. EFFECT OF BUOYANCY FORCE

In most studies it is assumed, that in the boundary layer the shear stress is constant $\tau = \tau_w = \text{const}$ which is a natural assumption in the boundary layer, where the buoyancy forces are neglected. However, if we want to consider the direction of vertical motion then we have to consider the influence of buoyancy forces on the velocity profile. Performing a force balance on imaginary element of liquid containing bubbles, (Fig. 4), we obtain the following force balance between the weight of the control volume $G = \rho_e g dx dy$ and the buoyancy force $B = \rho_l g dx dy$:

$$-d\tau_e dx + g \rho_l dy dx - \rho_e g dy dx = 0 \quad (30)$$

where $\rho_e = \rho_l(1-\alpha) + \rho_g\alpha$. From (30) we can derive the distribution of stress across the boundary:

$$\frac{d\tau_e}{dy} = -g \left(1 - \frac{\rho_g}{\rho_l}\right) \rho_l \alpha \quad (31)$$

As we see the solution for void fraction distribution requires solving of three differential equations (6), (18) and (31). Such an approach has not been found by the author in the open literature.

As can be seen suggested model consists of four differential equations in total. Equations describe the velocity profile (8), lateral velocity (25), void migration (28) and the shear stress distribution (31). Equation (6) is not explicit and presents numerical difficulties.

8. HEAT TRANSFER IN THE TWO-PHASE TURBULENT BOUNDARY LAYER

In the case of fully developed heat transfer in a two-dimensional boundary layer we obtain the energy balance equation, assuming constant physical properties $c_p = \text{const}$ and $\lambda = \text{const}$, in the form:

$$\frac{\partial}{\partial y} \left[(a + a_t) \frac{\partial T}{\partial y} \right] = 0 \quad (32)$$

From considerations that in the laminar sublayer there are only viscous effects and the turbulent ones are negligible we can determine the temperature drop across the layer, which in the non-dimensional form yields as follows:

$$T_w^+ - T_l^+ = \frac{q_w \nu_l \delta_l^+}{T_\infty \lambda u_\tau} = \frac{q_w \text{Pr} \delta_l^+}{T_\infty \rho c_p u_\tau} \quad (33)$$

In the buffer layer both influences of molecular and turbulent viscosity should be considered as well as molecular and turbulent thermal diffusivity. This gives us the following temperature drop across the buffer layer:

$$T_l^+ - T_p^+ = \frac{q_w}{\rho c_p u_\tau T_\infty} \frac{2\sigma_t}{\kappa} \ln \frac{2\sigma_t + \text{Pr} \kappa \delta_p^+ - 2\text{Pr}}{2\sigma_t + \text{Pr} \kappa \delta_l^+ - 2\text{Pr}} \quad (34)$$

Solution of the energy equation (32) is obtained after substitution of relevant velocity profile into the momentum equation, hence enabling determination of the turbulent viscosity and then solution of the temperature field.

In the present considerations we assume, that in the laminar and buffer sublayers there is merely a liquid flow, and hence the temperature drop is described by (33) and (34). Some changes will be applied only in the core of the flow, where the own model of two-phase flow will be used, where velocity profile is described by (8). Following the procedure used in determination of the temperature drop across the turbulent core in the case of the single phase flow, we can determine the corresponding temperature drop across the two-phase core region using the own model. It has the following non-dimensional form [23]:

$$\frac{dT^+}{dy^+} = -\frac{q \sigma_t u_\tau}{c_p \tau_w T_\infty} \frac{1}{\kappa y^+ (1-\alpha)^{0.5} + M \alpha \kappa^2 y^{+2}} \quad (35)$$

Assuming a constant heat flux and a constant shear stress boundary conditions we can obtain in this way the approximate temperature field in two-phase bubbly flow. Considered below are two cases.

8.1 Solution at constant void fraction across the boundary layer

Assuming a constant void fraction in the boundary layer on a plate equation (35) has an analytical solution in the form:

$$T^+ = \frac{q_w \sigma_t}{\rho c_p u_\tau T_\infty} \ln \left(\frac{(1-\alpha)^{0.5} + M \alpha \kappa y}{y} \right) + C \quad (36)$$

The constant C is determined from the boundary condition at the border of a laminar sublayer

$$y^+ = \delta_l^+ \quad T^+ = T_l^+ \quad (37)$$

Combining (36) and (37) we obtain the following solution

$$T^+ = T_l^+ + \frac{q_w \sigma_t}{c_p \rho u_\tau T_\infty} \ln \left(\frac{(1-\alpha)^{0.5} + M \alpha \kappa y^+ \delta_l^+}{(1-\alpha)^{0.5} + M \alpha \kappa \delta_l^+ y^+} \right) \quad (38)$$

In our first approach to determine temperature at the border of laminar sublayer let's assume that there are in the flow two zones, which intersect at the point of $y^+=11.6$, see Fig. 4. In the case of greater values of y^+ we are dealing with the turbulent flow, and for lower ones we have a laminar flow. Substitution of T_1 determined from (33) into (38) gives:

$$T^+ = T_w^+ - \frac{q_w \nu \delta_l^+}{T_\infty \lambda u_\tau} + \frac{q_w \sigma_t}{c_p \rho u_\tau T_\infty} \ln \left(\frac{(1-\alpha)^{0.5} + M \alpha \kappa y^+ \frac{\delta_l^+}{y^+}}{(1-\alpha)^{0.5} + M \alpha \kappa \delta_l^+ \frac{\delta_l^+}{y^+}} \right) \quad (39)$$

In order to determine the wall temperature T_w we may use another boundary condition, namely:

$$y^+ = \delta \quad T^+ = T_\infty^+ \quad (40)$$

The wall temperature takes then a form

$$T_w^+ = 1 + \frac{q_w \text{Pr} \delta_l^+}{T_\infty c_p \rho u_\tau} - \frac{q_w \sigma_t}{c_p \rho u_\tau T_\infty} \ln \left(\frac{(1-\alpha)^{0.5} + M \alpha \kappa \delta^+ \frac{\delta_l^+}{\delta^+}}{(1-\alpha)^{0.5} + M \alpha \kappa \delta_l^+ \frac{\delta_l^+}{\delta^+}} \right) \quad (41)$$

The resulting Nusselt number after small re-arrangements yields:

$$Nu = \frac{\alpha \delta}{\lambda} = \frac{q_w \delta^+ \nu}{\lambda T_\infty (T_w^+ - 1) u_\tau} = \frac{\delta^+ \text{Pr}}{\text{Pr} \delta_l^+ - \frac{\sigma_t}{\kappa (1-\alpha)^{0.5}} \ln \left(\frac{(1-\alpha)^{0.5} + M \alpha \kappa \delta^+ \frac{\delta_l^+}{\delta^+}}{(1-\alpha)^{0.5} + M \alpha \kappa \delta_l^+ \frac{\delta_l^+}{\delta^+}} \right)} \quad (42)$$

In the case of division of the boundary layer into three zones and implementing the procedure described above we can obtain the Nusselt number in the form:

$$Nu = \frac{\delta^+ \text{Pr}}{\text{Pr} \delta_l^+ + \frac{2\sigma_t}{\kappa} \ln \frac{2\sigma_t + \text{Pr} \kappa \delta_p^+ - 2\text{Pr}}{2\sigma_t + \text{Pr} \kappa \delta_l^+ - 2\text{Pr}} - \frac{\sigma_t}{\kappa (1-\alpha)^{0.5}} \ln \left(\frac{(1-\alpha)^{0.5} + M \alpha \kappa \delta^+ \frac{\delta_p^+}{\delta^+}}{(1-\alpha)^{0.5} + M \alpha \kappa \delta_p^+ \frac{\delta_p^+}{\delta^+}} \right)} \quad (43)$$

Both forms of solutions (42) and (43) are relatively simple for the description of this kind of phenomena and seem to be applicable for engineering calculations. From the analysis of the form of the Nusselt number it results that it is generally a function of the following independent parameters:

$$Nu = Nu \left(\frac{\text{Re}_\delta}{w_\infty^+}, M, \alpha, \text{Pr} \right) \quad (44)$$

Analysis of the above parameters on the Nusselt number will be presented later in the text.

8.2 Solution at variable void fraction

In the case of a variable void fraction presented above procedure unfortunately does not hold. The velocity profile (8) must be solved with equations describing the void fraction distribution (25) and (28). From the presented above procedure it results that in order to determine the temperature field in a two-phase flow with a variable void fraction we must solve simultaneously three ordinary differential equations with three unknowns. Calculations start at the border of the turbulent layer, with the boundary conditions:

$$y^+ = \delta \quad u^+ = u_\infty^+ \quad T^+ = 1 \quad \alpha = \alpha_\infty \quad \mathcal{G}_b^+ = \mathcal{G}_{b\infty}^+ \approx 0 \quad (45)$$

9. COMPARISON AGAINST EXPERIMENTAL DATA

Calculations performed using the postulated model have been compared against the experimental data of Marié et al. [9] for the case of upward bubbly flow on a flat plate. Calculations have been performed using the Mathcad7 software with adaptive stepsize.

In present calculations it has been assumed that in the equation (28), consisting of two contributions to bubble rotation, a contribution coming from the non-uniform lateral distribution of the bubbles, i.e. the rotation described by (14), has a much stronger influence and for that reason circulation coming from the velocity profile distribution was found to have little effect and has been neglected in present calculations. It has been done so due to the fact that the velocity profile in the boundary layer is flat for almost the entire region and has a strong variation only very close to the wall, where bubbles are not present and so the postulated theory. This term included in calculations causes significant numerical problems.

Calculations have been performed for one case corresponding to the experimental conditions. In the calculation of the equivalent velocity profile using the proposed model, the distribution of the void fraction from experiment corresponding to the external boundary layer void fraction value of 1.3% has been used (Fig. 5). Velocity distribution has been calculated using two methods, namely using the equation (9) ($\alpha = \text{const}$) and alternatively by simultaneous

solution of (8), (25) and (28) ($\alpha=\text{var}$). In calculations using equation (9) a constant value of $\alpha=1.3\%$ has been assumed and external liquid velocity was 1 m/s. The parameter M has been estimated to be $M=0.729$, which has been obtained for the spherical bubbles with the diameter of about $d_b=3.5$ mm. Obviously, in general, this parameter is variable with the distance from the wall, but a more detailed study of that influence has not been the merit of the present work. Velocity distribution obtained using the present model in comparison against the experimental data is presented in Fig. 7. In the figure presented are also the curves showing the single phase velocity profile. In Fig. 8 presented are calculations performed using various turbulence models for the case of single phase flow past the plate, along with the data for the external void fraction equal to 1.3%. As can be noticed a small influence of void fraction changes the picture of the flow. Predictions for the single phase flow differ significantly from the experimental data. In this light the predictions using the model show significantly improved consistency.

As can be seen from Fig. 7 and 8, a new simple model leads to surprisingly good results. There is, however, a quantitative discrepancy between the experiment and results of calculations, which is strongly influenced by the choice of the boundary condition on the velocity profile. The boundary condition assumed in Fig. 4 for the velocity profile was that for $w^+=y^+=8$. One of the objectives of the work would be to determine the error incurred from the asymptotic solution, which in the presented case does not exceed 10% in the core region.

From the analysis of Fig. 9 it results that in the location where the void fraction has its peak there is a change of sign of lateral velocity (Fig. 10), which supports entirely the theory described above.

In the case of core peaking the mechanism described above is also revealed (see Fig. 11 and 12). This means that in order to have a continuously increasing void fraction we need a negative value of bubble lateral velocity. This means that in such case bubbles travel towards the wall. Experimental data confirming such phenomenon are still unavailable yet in the literature.

Calculations of heat transfer were conducted for the following parameters:

- Heat flux density at the wall, $q_w - 100 \text{ kW/m}^2$,
- External fluid temperature $T_\infty - 300 \text{ K}$

- Film temperature for calculation of water physical properties – 300 K
($c_p=4190 \text{ J/kgK}$, $\lambda=0.6 \text{ W/mK}$, $\rho=1000 \text{ kg/m}^3$, $\nu=10^{-6} \text{ m}^2/\text{s}$)
- von Karman constant – 0.4
- Friction velocity corresponding to the experimental conditions [8] – $u_\tau=0.052 \text{ m/s}$
- Turbulent Prandtl number – $\sigma_t=1.0$

In calculations the following parameters were varied: the total boundary layer thickness δ^+ , i.e. the change of the Reynolds number of the flow, which can be defined as $Re_\delta = \delta^+ u_\tau / \nu$, bubble diameter d_b , i.e. the parameter M , and the void fraction α . Results are presented in the form of graphs in Fig. 13, 14 and 15, as well as in Tables 1, 2 and 3.

We can see from Fig. 13 that the increase of void fraction renders increase of temperature gradient in the boundary layer and hence the heat transfer coefficient. This is intuitively correct, as the presence of the bubbles intensifies heat transfer, but this finding tells us also, that the model gives a good qualitative agreement with practice. Values of the heat transfer coefficient for different void fractions are given in Table 1. It can be seen that both formulations, in the case of a two-zone model and a three-zone model, observe an increase of about 10% with the change of void fraction from 0 to 0.1. There is however, a significant quantitative discrepancy between the results given by the two- and three-zone models. In the case of the presence of bubbles in the flow we can see that the suggested model predicts almost zero temperature gradient for $y^+ > 400$, i.e. we can talk about the decrease of the thickness of the boundary layer due to the presence of bubbles. Single-phase flow predicts some temperature gradient at the border of the boundary layer.

In Fig. 14 presented is the influence of bubble diameter on the temperature distribution in the case where $\alpha=0.015$ and $\delta^+=1200$. A very important finding from Fig. 14 is that the smaller bubbles intensify more the heat transfer. This means that smaller bubbles turbulise more the boundary layer which is obvious. In the presented example the effect of the bubble diameter influence is of the order of 10%, in the considered range of bubble diameters.

In Fig. 15 and Table 3 presented is the influence of non-dimensional boundary layer thickness on heat transfer in the boundary layer. In this case the influence is not very significant, however it can be said that the thinner the boundary layer is the more intensified heat transfer becomes. The thinner boundary layer corresponds to larger external liquid velocities, which is consistent with the findings from single-phase flows.

In Fig. 16 presented are comparisons of calculations of temperature profiles obtained from the model based on a constant and variable void fractions for the case of experimental void fraction presented in Fig. 7 and 8. As can be seen the qualitative agreement is very good indeed. Void fraction, calculated using own model, has been substituted into the temperature field profile and in this way the temperature field had been determined. Calculated in such way temperature distribution has been compared against the temperature distribution calculated using equation (36) at constant void fraction equal $\alpha=1.3\%$. Calculations of heat transfer coefficient using a variable formulation predict higher values than the constant void fraction formulation. This is logical, as when we look at the void fraction distribution in Fig. 9 we can see the peak in its distribution, which takes a value of about 6.5%, and hence the heat transfer must be more intensified in this location. Summarising, it can be said that the proposed model has a good qualitative and quantitative agreement as far as hydrodynamics is concerned, which allows to judge that the similar should hold in the case of heat transfer in two-phase flow on a plate.

10. CONCLUSIONS

In the paper author's own model of bubbly flow in the boundary layer has been presented. The model is based on two hypothesis, namely the first one based of summation of dissipation resulting from liquid flow and presence of bubbles. The second hypothesis presented in the paper is identification of additional circulation around bubble, which in author's opinion is responsible for different gathering of bubbles in the flow, i.e. wall peaking and core peaking. The results obtained using such model have been confronted against experimental data, where satisfactory agreement has been achieved. That confirmed the appropriateness of assumed hypothesis. Formulated and presented model of bubbly flow without bubble generation in its general form consists of four differential equations of the first order, namely: equation of lateral bubble velocity, lateral distribution of void fraction, shear stress distribution and equivalent velocity of two-phase flow. It is worth stressing that in the case of a constant void fraction distribution its is possible to obtain analytical form of velocity profile, which can be regarded as some kind of the law of the wall. In author's opinion such model can be disseminated for a wider use amongst engineers. Due to two contributions of circulation around the bubble the model is capable of predicting the phenomena of wall peaking and core peaking. In the case of wall peaking, there must be a change of the sign of void fraction

gradient in the peak, which renders that at this location there must be a change of a sign of lateral velocity. Presented model can restore this phenomenon. In the case of core peaking we deal with a negative value of lateral velocity, which means that it is directed towards the wall.

In the paper presented also is author's own solution to heat transfer in bubbly flow. Again, two solutions have been presented. The first one, analytical, has been obtained for the case of bubbly flow with the constant distribution of void fraction. Obtained analytical temperature distribution in the boundary layer may quite useful to engineering practice due to a reasonable accuracy, if compared against the solution incorporating variable distribution of void fraction. The second solution, more accurate, is based on solution of a set of five differential equations, namely: lateral distribution of void fraction, lateral velocity, shear stress distribution, equivalent flow velocity and temperature. However it is a more accurate solution it requires more complex numerical calculations.

Summarising it can be concluded, that despite intensively conducted experimental, theoretical and numerical works in the area of two-phase flows more research is still requires into understanding of bubbly flows. Presented in the paper model shows, in author's own opinion, directions for further research on understanding of a complex nature of two-phase flows.

ACKNOWLEDGEMENTS

Author expresses his gratitude to the State Committee for Scientific Research for funding his grant PB 7 T07A 048 12

LITERATURE

1. Drew D.A. and Wallis G.B., Fundamentals of Two-Phase Flow Modeling, in Multiphase Science and Technology, Vol. 8, 1-67, ed. G.F. Hewitt et al., Begell House inc., New York, 1994.
2. Lance M, Lopez de Bertodano M., Phase Distribution Phenomena, in Multiphase Science and Technology, Vol. 8, 69-123, ed. Hewitt et al., Begell House inc., New York, 1994.
3. Lahey R.T. Jr, Drew R.T., The analysis of two-phase flow and heat transfer using a multidimensional, four field, two-fluid model, Nuclear Engineering and Design, 204, 29-44, 2001.
4. Serizawa A., Kataoka I., and Michiyoshi I., Turbulence structure of air-water bubbly flow, Int. J. Multiphase Flow, 2, 221-259, 1975.
5. Wang SK, Lee SJ, Jones OC Jr, Lahey RT Jr, Three-Dimensional Turbulence Structure and Phase Distribution Measurements in Bubbly Two-Phase Flows, Int. J. Multiphase Flow, 13, 327-343, 1987.
6. Nakoryakov V.E., Kashinsky O.N., Burdukov A.P. and Odnoral V.P., Local characteristics of upward gas-liquid flows, Int. J. Multiphase Flow, Vol. 7, 63-81, 1981.
7. Liu T.J., Bubble size and entrance length effects on void development in a vertical channel, Int. J. Multiphase Flow, Vol. 19, 99-113, 1993.
8. Moursali E., Marié JL and Bataille J., An upward turbulent bubbly boundary layer along a vertical flat plate, Int. J. Multiphase Flow, Vol. 21, No. 1, 107-117, 1995.
9. Marié JL, Moursali E, Tran-Tong S., Similarity law and turbulence intensity profiles in a bubble layer at low void fractions, Int. J. Multiphase Flow, Vol. 23, 227-247, 1997.
10. Mikielewicz D., A new model of a turbulent two-phase disperse flow in the boundary layer, Proc. 2nd Int. Symp. on Two-Phase Flow Modelling and Experimentation, Pisa, Italy, 23-26 May, 1999.

11. Mikielewicz D., Universal velocity profile in bubbly flow in the turbulent boundary layer, *Archives of Thermodynamics*, Vol. 21, No. 3-4, 2000, 117-132.
12. Mikielewicz D., A New Model of Bubble – Liquid Interaction in the Boundary Layer, *Proc. 2nd Int. Conference on Heat Transfer and Transport Phenomena in Multiphase Systems*, 18-22 May 1999, Kielce, Poland.
13. Lance M., Marié J.L., Bataille J., Homogeneous turbulence in bubbly flows, *J. of Fluid Engineering*, 113, 295-300, 1991.
14. Polyani A.D., Dilman V.V., *Methods of modeling equations and analogies in chemical engineering*, CRC Press Inc. Boca Raton, Florida, 1994.
15. Troshko A.A., Hassan Y.A., law of the wall for two-phase turbulent boundary layers, *Proc. of 11th Int. Heat Transfer Conference*, Vol. 2, pp. 139-145, Kyongju, Korea, 1998.
16. Moraga F.J., Bonetto F.J., Lahey R.T., Lateral forces on spheres in turbulent uniform shear flow, *Int. J. Multiphase Flow*, 25, 1321-1372, 1999.
17. Mikielewicz D., Added mass in the lateral motion of bubbles in the boundary layer, *Proc. X Polish-German Symposium Research-Practice-Education*, Gdańsk, 18-19 May 2000.
18. Madejski J., Vapour departure conditions in flow boiling, *Transactions of IFFM*, 1968.
19. Žun I., The transverse migration of bubbles influenced by walls in vertical bubbly flow, *Int. J. Multiphase Flow*, vol. 6, 583-588, 1980.
20. Sir Horace Lamb, *Hydrodynamics*, 7th ed. Cambridge University Press, 1972.
21. Bankoff S.G., A variable density single-fluid model for two-phase flow with particular reference to steam-water flow, *J. Heat Transfer*, 82, 265-270, 1960.
22. Tomiyama A., Kataoka I., Žun I. and Sakaguchi T., Drag Coefficients of Single Bubbles under Normal and Micro Gravity Conditions, *JSME Int. J., Ser. B*, 41, 2, 1998.
23. Mikielewicz D., Modelling of heat transfer in bubbly flow in the turbulent boundary layer, *Archives of Thermodynamics*, Vol. 22, No. 1-2, 33-49, 2001.

Table 1 Comparison of the values of heat transfer coefficient with respect to void fraction using a two-zone and three-zone models ($M=0.73$, $\delta^+=1200$). Indices denote: m2l – proposed two-zone model, m3l – proposed three-zone model; 2l –theoretical two-zone single phase model, 3l – theoretical three-zone single phase model.

THREE-ZONE MODEL					
Void fraction	$T_w^+{}_{m3l}$	$T_w^+{}_{3l}$	α_{m3l}	α_{m3l}/α_{3l}	Nu_{m3l}
[%]	[-]	[-]	W/m ² K	[-]	[-]
0	1,047	1.047	3512	1.000	135.06
1.5	1,044	1.047	3770	1.073	144.99
3.0	1,043	1.047	3853	1.097	148.183
5.0	1,043	1.047	3912	1.114	150.477
7.5	1,042	1.047	3956	1.126	152.156
10.0	1,042	1.047	3984	1.134	153.234

Table 2 Influence of bubble diameter on heat transfer in the boundary layer (three-zone model), $\alpha = 0.015$, $q=100000$ W/m².

Parameter	d_b	$T_w^+{}_{m3l}$	α_{m3l}	Nu_{m3l}
M	[mm]	[-]	W/m ² K	[-]
11.2	0.50	1.08231	4050	155.760
6.22	0.75	1.08317	4008	154.142
4.132	1.0	1.08395	3970	152.709
1.569	2.0	1.08630	3863	148.563
0.73	3.5	1.08842	3770	144.993
0.45	5.0	1.08974	3714	142.855
0.26	7.5	1.09112	3658	140.703

Table 3 Influence of non-dimensional boundary layer thickness (Reynolds number) on heat transfer in the boundary layer (three-zone model).

δ^+	$T_w^+_{m3l}$	$T_w^+_{3l}$	α_{m3l}	α_{3l}	Nu_{m3l}	Nu_{3l}
[-]	[-]	[-]	W/m ² K	W/m ² K	[-]	[-]
250	1,08660	1,09552	3849	3749	30,842	27,961
500	1,08765	1,09552	3803	3640	60,948	55,921
1000	1,08830	1,09410	3775	3538	120,993	111,843
1200	1,08842	1,09500	3770	3512	144,993	134,211
2000	1,08867	1,09700	3759	3441	240,965	223,685
2500	1,08875	1,09800	3756	3411	300,937	279,607

Figure captions:

Fig. 1. Forces acting on the bubble in vertical flow

Fig. 2. Model of two-phase flow

Fig. 3 The model of bubble moving through liquid.

Fig. 4 Force balance on the two-phase element of fluid.

Fig. 5. Two-zone boundary layer

Fig. 6 Three-zone boundary layer.

Fig. 7 Velocity distribution at void fraction $\alpha=1.3\%$

Fig. 8 Velocity distribution calculated using various turbulence models at void fraction $\alpha=1.3\%$

Fig. 9 Void fraction distribution in upward flow – wall peaking.

Fig. 10 Lateral velocity distribution in upward flow – wall peaking case.

Fig. 11 Void fraction distribution in upward flow – core peaking.

Fig. 12 Lateral velocity distribution in upward flow – core peaking case.

Fig. 13. Influence of void fraction on temperature distribution in the boundary layer (three zone model). $M=0.73$, $\delta^+=1200$, $q_w=100000\text{W/m}^2$.

Fig. 14 Influence of bubble diameter on temperature distribution in the boundary layer. $\alpha=0.015$, $M=0.73$, $\delta^+=1200$, $q_w=100000\text{ W/m}^2$.

Fig. 15 Influence of non-dimensional boundary layer thickness on heat transfer in the boundary layer. $\alpha=0.015$, $M=0.73$ ($d_b=3.5\text{ mm}$).

Fig. 16 Comparison of theoretical temperature distribution using the model at constant void fraction and the variable void fraction formulation.

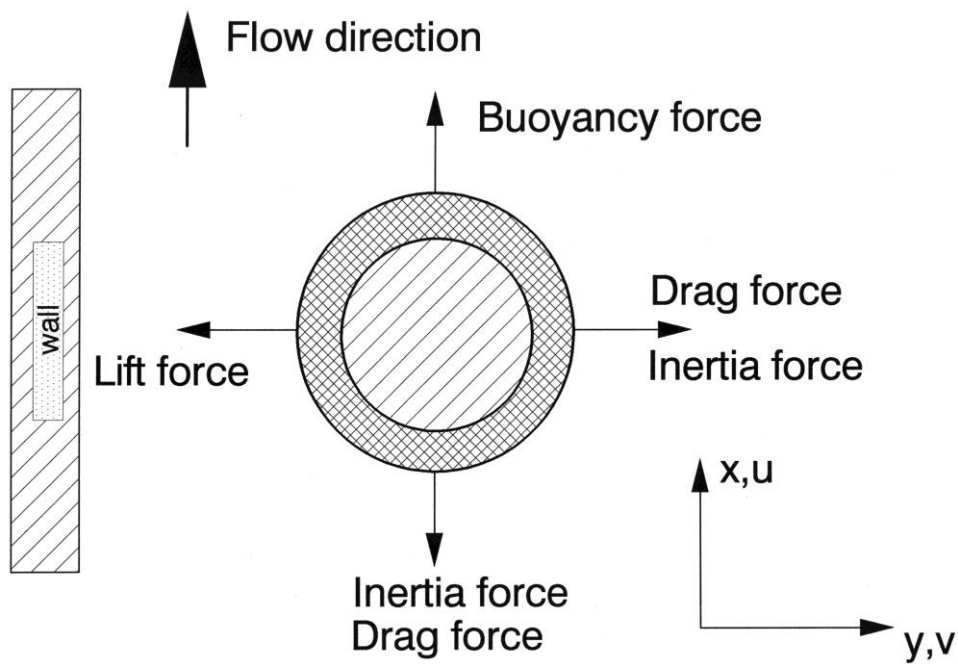


Fig. 1. Forces acting on the bubble in vertical flow

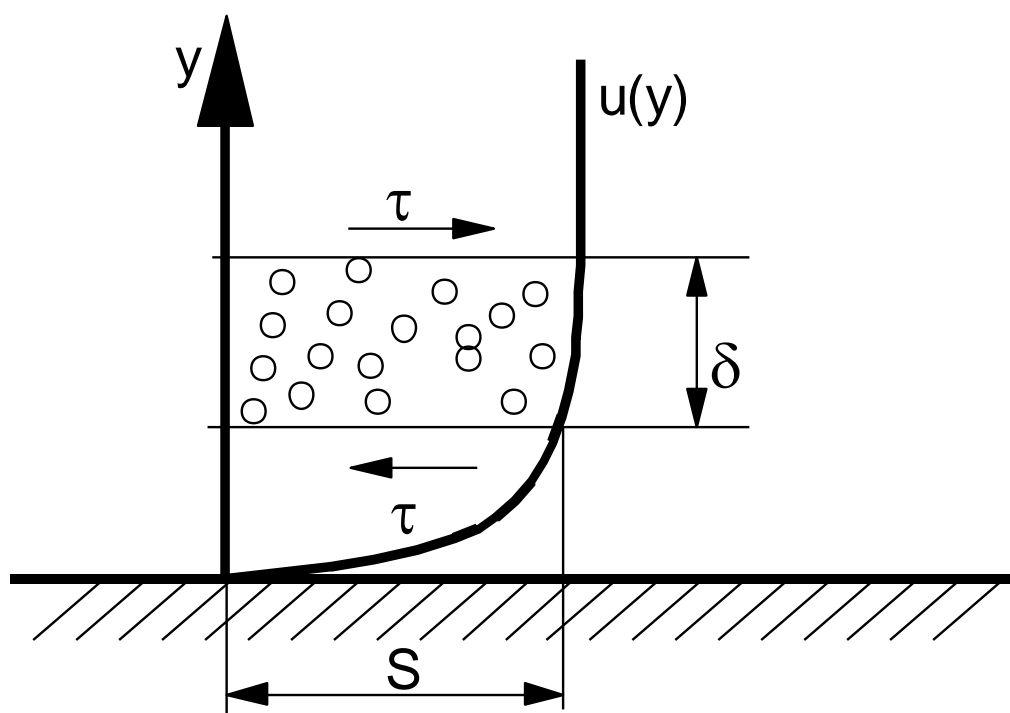


Fig. 2. Model of two-phase flow

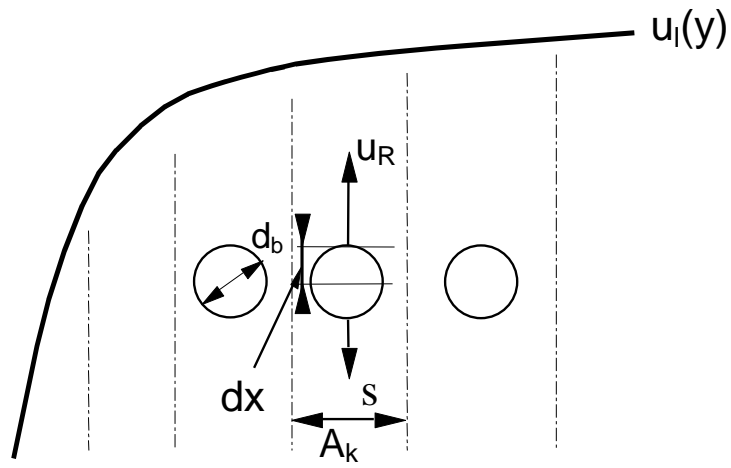


Fig. 3 The model of bubble moving through liquid.

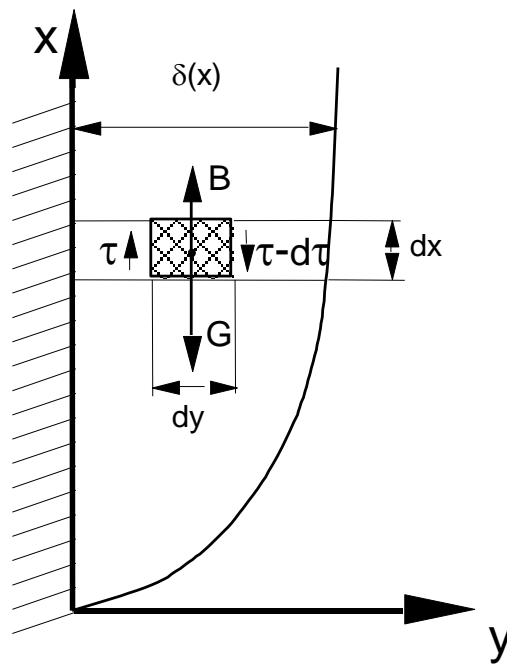


Fig. 4 Force balance on the two-phase element of fluid.

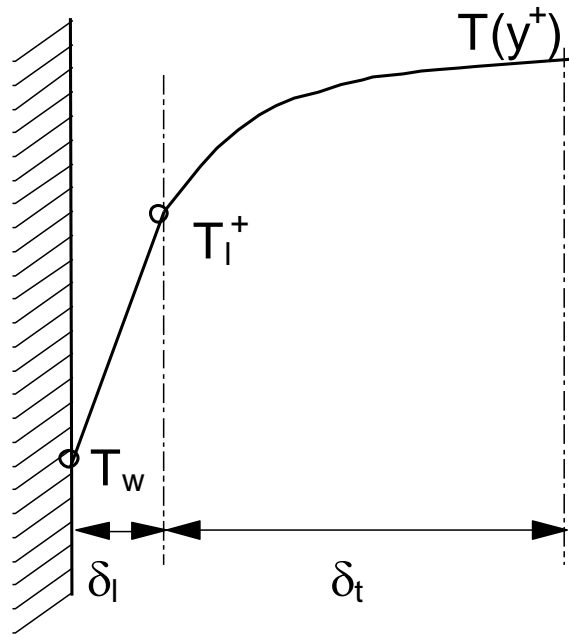


Fig. 5. Two-zone boundary layer

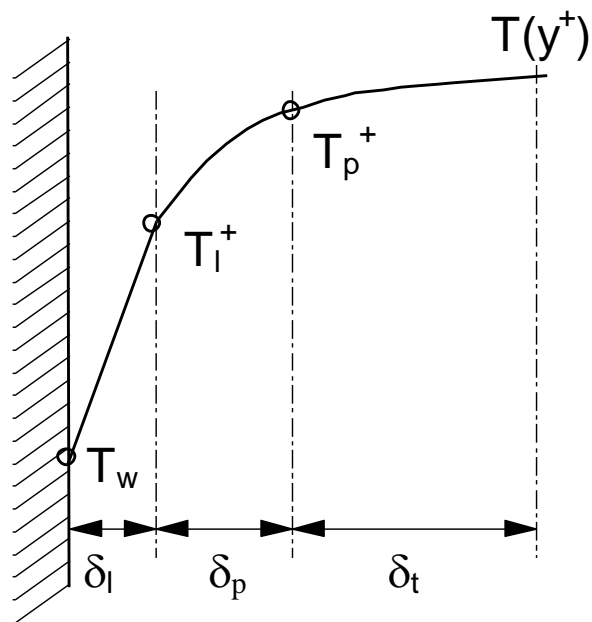


Fig. 6 Three-zone boundary layer.

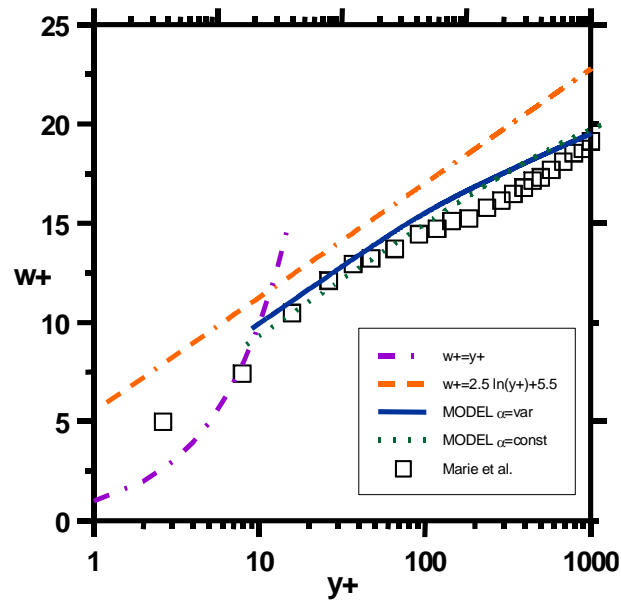


Fig. 7 Velocity distribution at void fraction $\alpha=1.3\%$

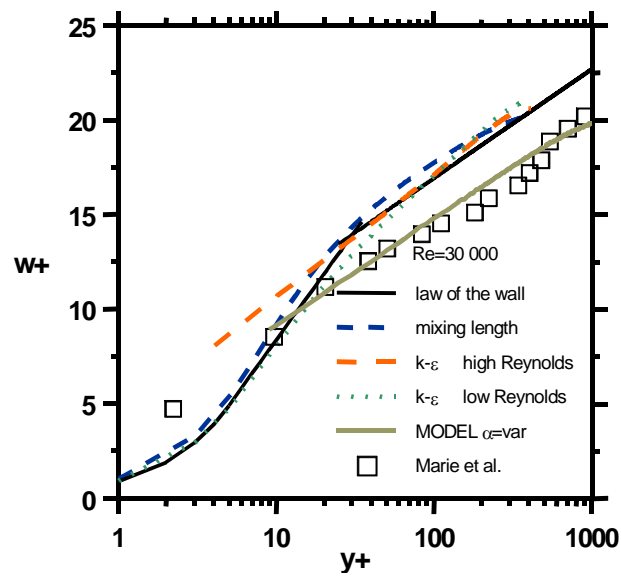


Fig. 8 Velocity distribution calculated using various turbulence models at void fraction $\alpha=1.3\%$

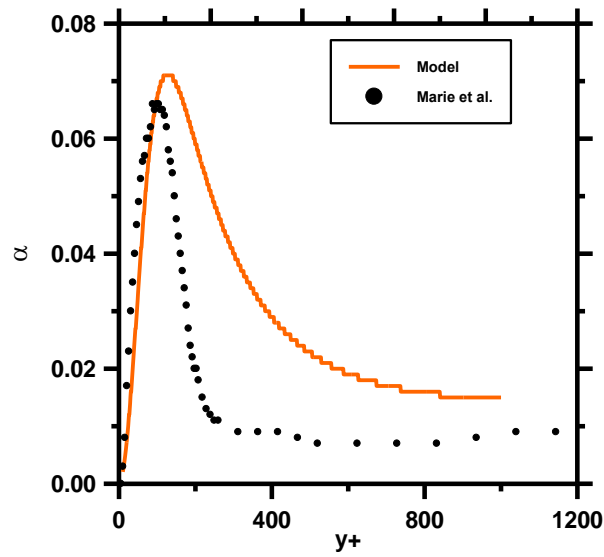


Fig. 9 Void fraction distribution in upward flow – wall peaking.

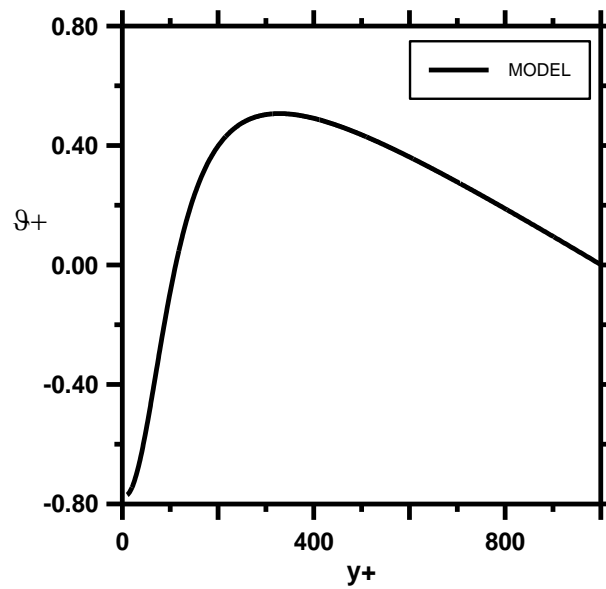


Fig. 10 Lateral velocity distribution in upward flow – wall peaking case.

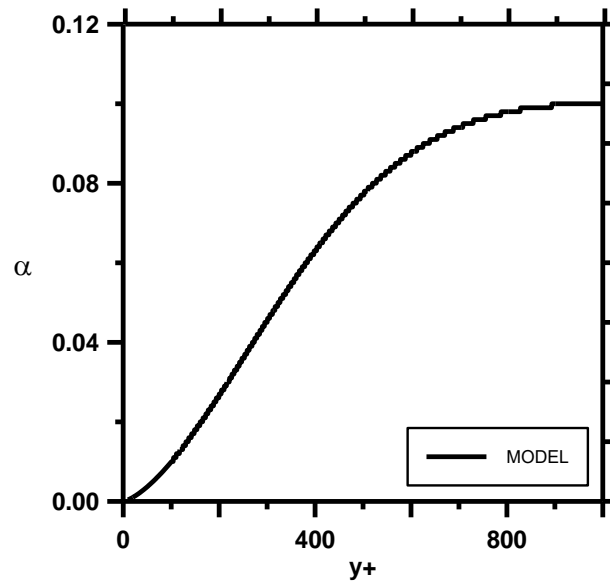


Fig. 11 Void fraction distribution in upward flow – core peaking.

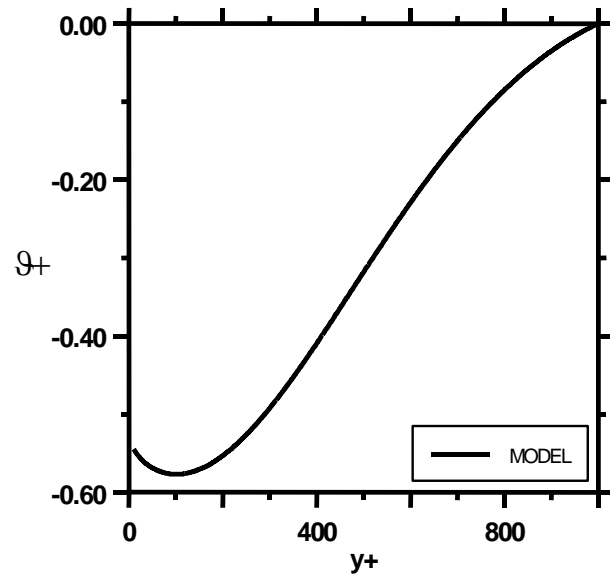


Fig. 12 Lateral velocity distribution in upward flow – core peaking case.

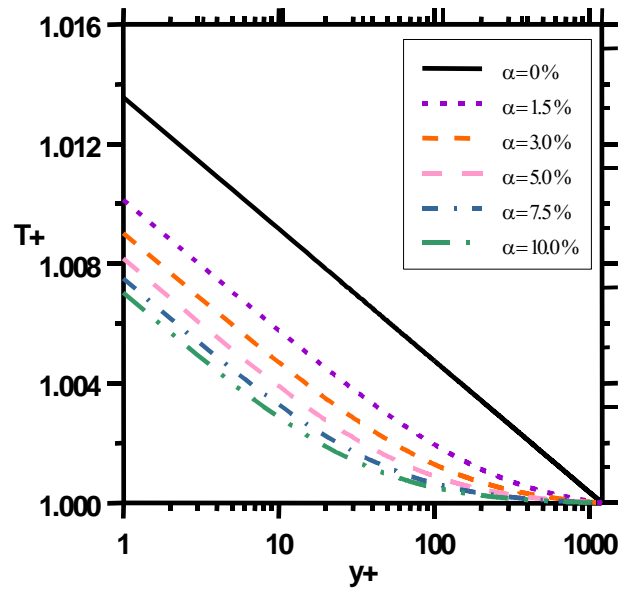


Fig. 13. Influence of void fraction on temperature distribution in the boundary layer (three zone model). $M=0.73$, $\delta^+=1200$, $q_w=100000\text{W/m}^2$.

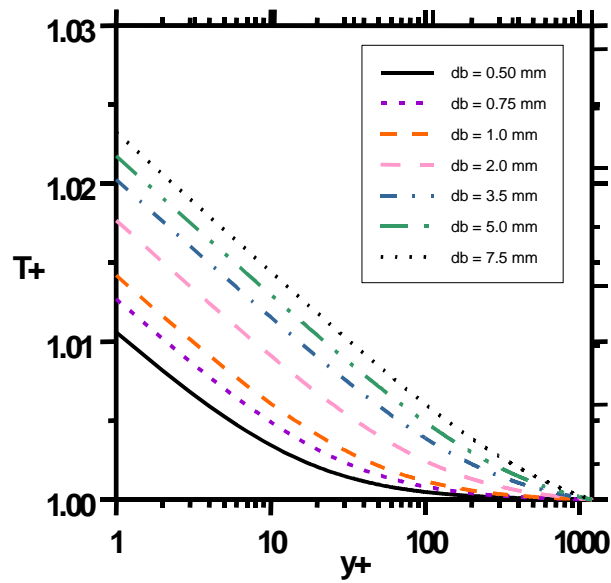


Fig. 14 Influence of bubble diameter on temperature distribution in the boundary layer. $\alpha=0.015$, $M=0.73$, $\delta^+=1200$, $q_w=100000\text{ W/m}^2$.

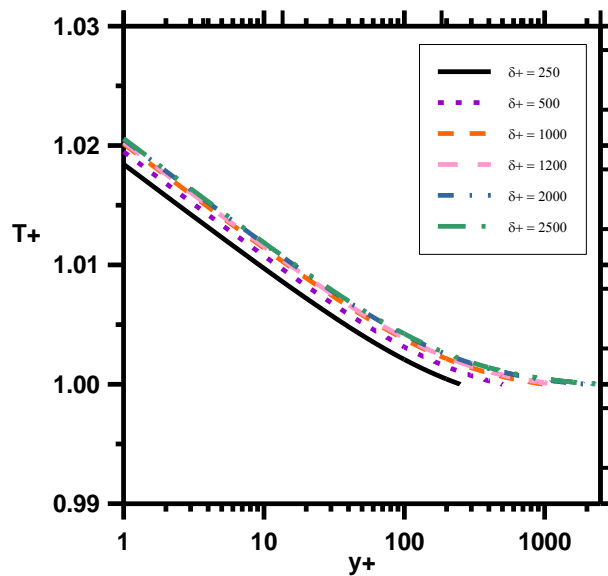


Fig. 15 Influence of non-dimensional boundary layer thickness on heat transfer in the boundary layer. $\alpha=0.015$, $M=0.73$ ($d_b=3.5$ mm).

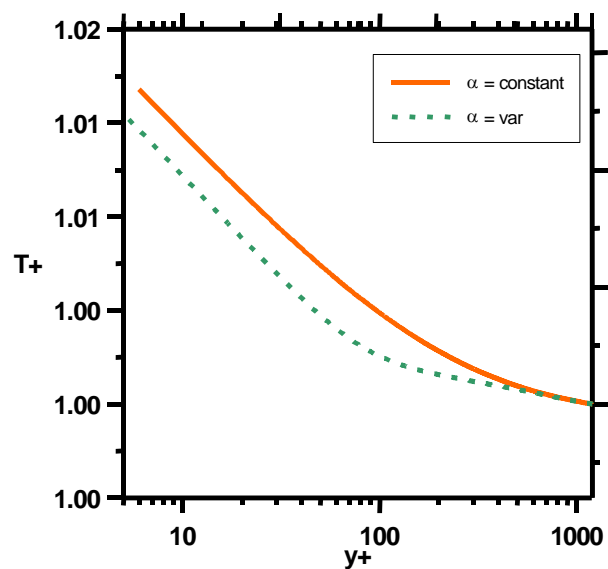


Fig. 16 Comparison of theoretical temperature distribution using the model at constant void fraction and the variable void fraction formulation.